Strength and Toughness of Bone-Shaped Steel Wire Reinforced Cement

Hongang Jiang, James A. Valdez, Y. Theodore Zhu, Irene J. Beyerlein and Terry C. Lowe

MS G755, Materials Science and Technology Division,
Los Alamos National Laboratory, Los Alamos, New Mexico 87545
Submitted to Composite Science and Technology
LAUR# 99-4654

Abstract

In this study, we experimentally evaluated the effectiveness of bone-shaped short (BSS) steel wire reinforcement in improving the mechanical properties of cement. Results from four point bending tests revealed that BSS steel wire reinforced cement is substantially stronger, tougher, and more crack resistant than conventional straight short (CSS) steel wire reinforced cement and unreinforced cement. The BSS steel wires provided effective crack bridging by a combination of their ductility and the mechanical interlocking between their enlarged spherical ends and the brittle cement matrix. In the BSS-wire reinforced cement specimens, multiple cracks formed along the length of the specimen before final failure; whereas in the CSS-wire reinforced cement and unreinforced cement specimens, a single central crack initiated and propagated across the specimen. Some BSS wires bridged the main crack and were eventually plastically deformed to failure. Also secondary matrix cracks radiated away from the main fracture surfaces, providing significant contributions to the toughness of the composites. In contrast, the bridging CSS wires were easily pulled out of the matrix without much deformation in the wire itself and surrounding cement. Therefore, they were not nearly as effective in bridging crack and improving toughness as the BSS wires.

1. Introduction

Unreinforced concrete has low tensile strength and low toughness. This common structural material is usually used in civil engineering infrastructures such as sidewalks, streets, highways, stadiums, bridges and house foundations. Thermal stresses caused by temperature change, as well as service stresses, often cause cracks years later, after these concrete infrastructures are built. The major mechanical properties that affect the performance of a concrete infrastructure include first crack strength, maximum strength, and toughness. Concrete applications where safety is crucial, such as components in bridges and buildings, are often reinforced with high strength, ductile steel rebars to make the concrete crack-resistant, and improve overall strength and toughness. However, rebars must be manually tied together to create a framework before concrete is poured, which significantly increases the labor cost and construction time. Conventional straight short (CSS) fibers made of glass, polymer or steel have been recently used to reinforce concrete with some success [1-4]. Using short fiber-reinforced concrete reduces the amount of costly rebars and improves the overall mechanical properties of concrete infrastructures [5-7]. The advantage of CSS fibers is that they can be directly mixed with materials used in forming concrete, and therefore would not add any labor cost or additional construction time.

Materials reinforced with short discrete fibers (or wires) have been extensively studied for several decades [8-12]. The effectiveness of short fibers has been demonstrated in a variety of fiber-matrix systems [8-15], where constituent materials are polymeric, metallic, or ceramic. In nearly all systems, it has been a challenge to simultaneously increase the strength and fracture toughness of composite materials reinforced with short fibers. Increasing the strength of composite materials usually compromises material fracture toughness, or the capability of resisting crack propagation. High composite strength can be achieved by choosing an appropriate high strength fiber or ensuring a strong interface between the matrix and the fiber. However, a strong interface may result in lower toughness, because it does not allow interfacial debonding, a mechanism that relieves stress concentrations produced by an oncoming crack. Debonding also allows the crack to propagate around the fiber, leaving the fiber intact in its wake.

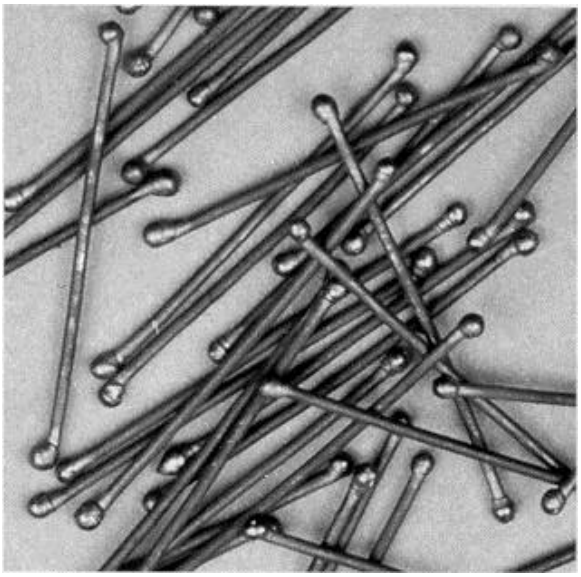

Figure 1. Bone-shaped steel wires. The wire length is 25 mm.

In many brittle matrix-ductile fiber reinforced composite systems, like the cement matrix-steel short fiber composite studied here, the interface is relatively weak. These short fibers in a composite can potentially bridge propagating cracks, consequently improving fracture toughness. Bridging short fibers in the wake of a crack can be debonded from the matrix, pulled out, stretched, broken, or reoriented, as the crack propagates. The type and combination of responses of the bridging short fibers as the crack surfaces displace determine the crack bridging forces and their ability to resist crack propagation. For instance, if the frictional resistance of the debonded fiber-matrix interface is very weak, and hence, the fibers easily pull-out, these forces will be small and not be effective in resisting crack propagation [16]. This is the case for the CSS fiber reinforced concrete. This explains why the CSS fiber concrete performance is still not satisfactory in resisting crack propagation, though providing some improvement in strength and toughness over blank concrete.

Recently, a novel approach of using bone-shaped short (BSS) fibers with two enlarged ends to reinforce materials has demonstrated potential in improving both the strength and toughness of materials significantly and simultaneously [16-19]. In these

previous studies, the composite systems were polymer fiber-polymer matrix, wherein the BSS fibers, bridging matrix cracks, were pulled out and did not fracture. In these cases, the primary toughening mechanism was large-scale deformation of the surrounding matrix as the enlarged fiber ends pulled out. In this work, we explore the potential of BSS steel wires, as shown in Fig. 1, to bridge cracks and to improve the toughness of concrete more effectively. Concrete is usually referred to a mixture of cement and aggregates. In this study, for simplicity, cement without aggregates is used as the composite matrix. Although the pure cement matrix may display less crack resistance than aggregate concrete, the results obtained from this study should still be applicable to the concrete since they both are brittle materials. For this system, we find that most BSS steel wires bridging matrix cracks plastically deformed, and in most cases, to the point of fracture.

The knowledge obtained from this study on short steel wire reinforced cement may be applicable to a broad range of ductile fiber reinforced brittle matrix composites. In such composite systems, toughness is usually the primary concern. If properly utilized, plastic deformation of the ductile reinforcement is one mechanism that can potentially increase the material toughness. The other mechanism for increasing toughness is fiber pull-out. By changing the reinforcement from CSS wire to BSS wires, we alter the dominant toughening mechanisms from the latter to the former. The enlarged ends of the BSS steel wires prevent these bridging wires from being pulled out of the cement matrix and enable them to deform plastically to failure.

The objective of this research is 1) to study the feasibility of using BSS steel wires as an effective, low cost way for improving the toughness of concrete infrastructures, and 2) to study the effectiveness of plastic deformation of BSS wires over that provided by the pull-out of CSS wires in improving first crack strength, maximum strength, and toughness.

2. Experimental procedures

Three types of four-point bending test specimens, BSS steel wire reinforced cement, CSS steel wire reinforced cement and blank cement, were fabricated. These tests allowed us to identify and compare the roles played by discrete CSS and BSS wires on strengthening cement**.** The dimensions of the specimens were approximately 240 mm x 38 mm x 25 mm.

The short steel wires were made from commercial utility wires with a yield strength of 260 MPa, and a failure strain of 12.6%. Figure 2 shows the typical tensile stress-strain curve of these wires. Both BSS and CSS short wires have a diameter of 0.84 mm and a length of 25 mm. The BSS steel wires were made by first cutting the wire into a length of 28 mm and then melting both ends with a torch, resulting in enlarged wire ends with an average diameter of 1.6 mm (see Fig. 1).

The cement matrix was prepared by blending 210 ml water and 600 g Portland cement (water/cement ratio of 20/7 ml/g) until a uniform mixture was obtained. The water/cement ratio of 20/7 ml/g was determined by the fact that at this ratio the viscosity of the cement matrix is optimum for limiting the size and amount of air bubbles in the specimens while at the same time preventing the wires from sinking. In the case of unreinforced cement specimens, the cement/water mixture was directly poured into a mould, and the mould was shaken to ensure that the cement filled the mould fully and to release trapped air bubbles.

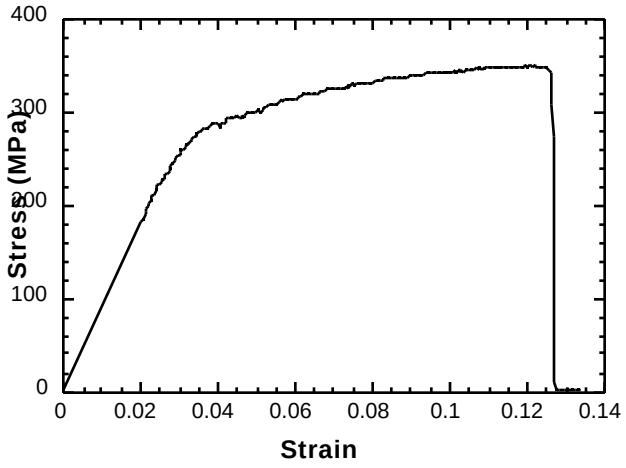

Figure 2. The stress-strain curves of steel wires.

For the fabrication of CSS and BSS steel wire reinforced cement, four layers of steel wires were carefully laid into the cement specimens, equally dividing the 25 mm thickness. The template used for manually laying steel wires in each layer is shown in Fig. 3. The template was flipped over about its longer side for each alternate layer to ensure a uniform distribution of wires. Such a wire arrangement prevents the alignment of wire ends of adjacent wires in the transverse direction. The alignment of wire ends may promote crack formation and propagation in the plane of alignment. With this scheme, the steel wire volume fraction was approximately 0.86 % and 1 % for the CSS- and BSS-wire reinforced specimens, respectively. The difference in volume fraction is caused by the enlarged ends of BSS wires.

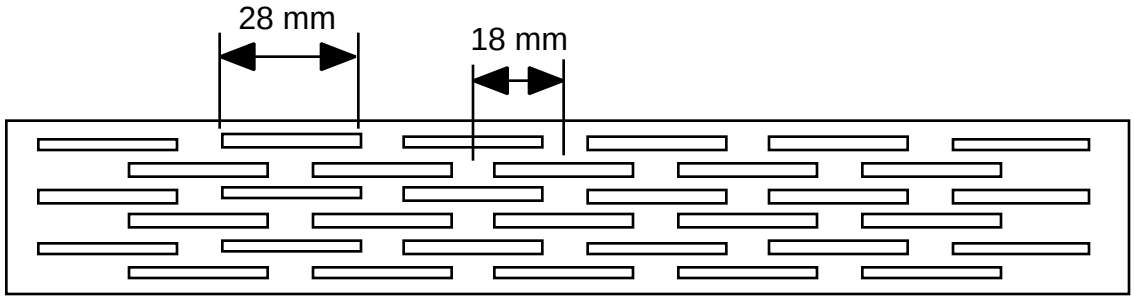

Figure 3. Schematic illustration of the template for manually laying steel wires.

For all three specimen types the curing was carried out in sealed plastic bags for 20 days and then in air for 15 days prior to the four point bend tests. This procedure prevented the loss of moisture during the curing process so that the chemical reactions between water and cement took place as expected. Otherwise, quick drying of the cement and insufficient curing time tend to dramatically reduce the strength of the cement because the reactions need water and are slow [20].

Four-point bending tests were used to examine the fracture properties of these cement specimens. The experimental test set-up is schematically shown in Fig. 4. During

the tests, a cross-head displacement rate of 0.5 mm/min was maintained; the evolution of the load as a function of the cross-head displacement was recorded.

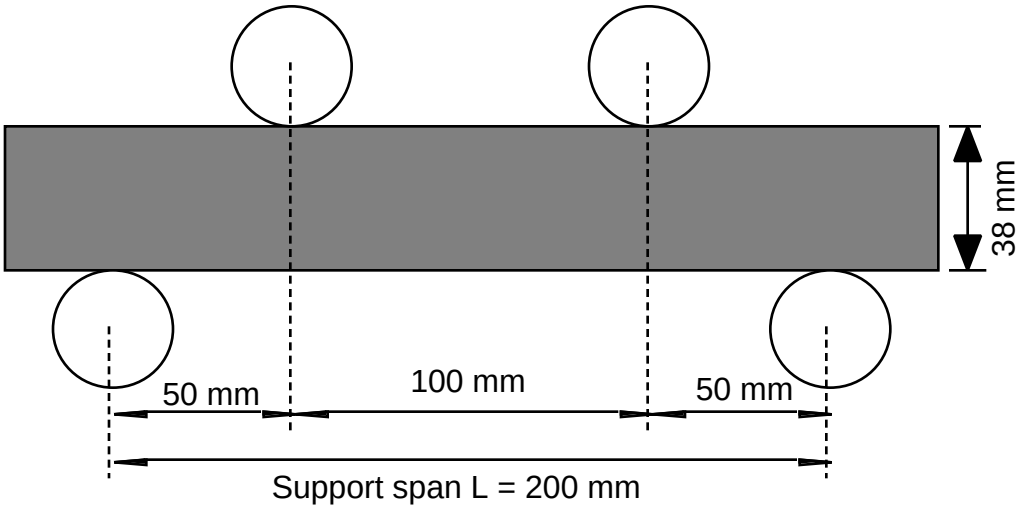

Figure 4. The setup of four-point bending flexural test.

3. Results

3.1 Load-Displacement Response

Figure 5 compares curves of the load P as a function of the cross-head displacement (hereafter simply referred to as displacement) typical of the unreinforced and CSS- and BSS-wire reinforced specimens. From these curves, the *first crack point,* defined as the point on the load-displacement curve at which the form of the curve first becomes nonlinear [4]; the maximum load, P_m; and the apparent toughness, are of interest. The apparent toughness is calculated as the area under the load-displacement curve. Consequently, toughness is defined hereafter as the total energy consumed by the specimen up to complete failure. Since all specimens in this study have the same dimension, it is valid to use this definition of toughness for comparison.

The curve for the unreinforced cement displays typical brittle fracture behavior with a maximum load of 965 N at a displacement of 0.19 mm. This maximum load also coincides with the first crack load, P_1, where a single crack formed around the midpoint of the specimen and promptly propagated and failed the specimen. The immediate failure of the whole specimen after the initiation of the crack led to a low toughness of only 0.08 J (Fig. 5).

The curve for the CSS steel wire reinforced cement specimen indicated improvements in mechanical properties over that of the unreinforced cement. A careful examination of the curve reveals a sharp change of slope at a load of 1185 N. This was

caused by the initiation of the first crack. Therefore, the addition of 0.86 vol. % CSS steel wires increased the load of the first crack point by 22.8%. After initiation of the first crack, the load continues to increase quickly with increasing displacement until it reaches a maximum load of 1280 N. This yields an increase in the P_m by 32.3% over the unreinforced specimen. Quick growth of the first crack caused the steady drop in load after the P_m. The general feature of this curve is typical of CSS steel wire reinforced concrete [1, 21, 22].

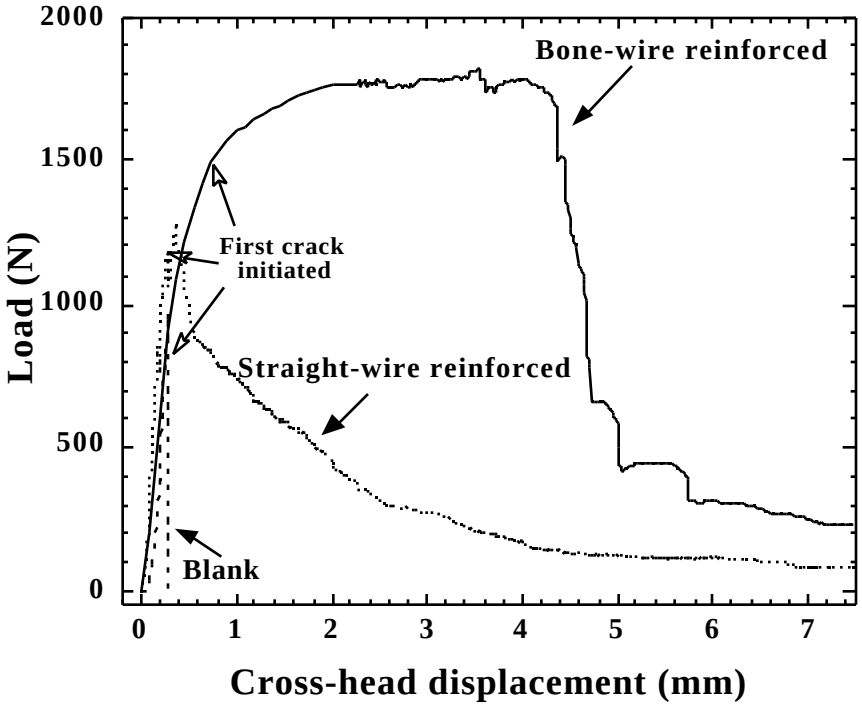

Figure 5. Load as a function of cross-head displacement for unreinforced and BSS- and CSS-steel wire reinforced concrete specimens.

Note that the descending portion of the load-displacement curve, after P_m is reached, is very similar to that of the pull-out curve [23-25] of a single CSS wire. This suggests that crack propagation after the formation of the first crack was dominated by the debonding and pull-out of the steel wires. The CSS steel wires enable the specimen to retain some degree of structural integrity and post-crack resistance, which significantly improves the toughness over that of the unreinforced cement. The toughness of the CSS steel wire reinforced cement specimen is 2.11 J, which is 26 times that of the unreinforced specimen.

Also shown in Fig. 5 is the curve for the BSS steel wire reinforced cement specimen, which is remarkably different from those for the unreinforced and CSS steel

wire reinforced cement specimens. The first crack was initiated at 1500 N, an increase of 55.4% over the unreinforced cement. After the first crack point, the load continued to increase gradually with increasing displacement until it reached a plateau of 1780 N. This load plateau was maintained up to a displacement of 4.3 mm, beyond which the load dropped sharply. The sharp drop in load at the end of the plateau was caused by the fracture of the BSS wires bridging the main crack. In addition, a few smaller abrupt load drops were observed, possibly caused by the fracture of individual BSS steel wires. This response illustrates the superior crack-bridging capability of BSS steel wires. The toughness of the BSS steel wire reinforced cement specimen is 7.62 J, which is ~94 times that of the unreinforced specimen and 3.6 times that of the CSS steel wire reinforced cement specimen. Therefore, BSS steel wires are significantly more effective than CSS steel wires in increasing both the strength and the toughness of blank cement. Note that these improvements occur with a mere 1.0 vol.% BSS steel wire. As suggested by the initial slopes of the curves shown in Fig. 5, this volume percent of reinforcement does not significantly alter the cement stiffness.

Flexural strength is one of the most important material properties in designing concrete infrastructure. For the four-point bending test shown in Fig. 4, the flexural strength S can be calculated as [26]

$$S = \frac{3PL}{4wh^2} \tag{1}$$

where P is the load, L is the span length; w and h are the width and the height of the specimen, respectively.

TABLE 1 The load (P_1), flexural strength (S_1) and displacement (D_1) at the initiation of the first crack, maximum load (P_m) and flexural strength (S_m), and toughness (G) obtained from four-point bending tests for unreinforced cement, CSS wire reinforced cement and BSS wire reinforced cement specimens. The wire volume fraction is 0.86 vol.% and 1.0 vol. % for CSS- and BSS-steel wire reinforced cement specimens, respectively.

Mechanical Properties	Unreinforced cement	CSS wire reinforced cement		BSS wire reinforced cement	
		Measured	Increase*	Measured	Increase*
P_1 (N)	965	1185	22.8%	1500	55.4%
D_1 (mm)	0.19	0.27	42.1%	0.75	294.7%
S_1 (MPa)	4.07	5.00	22.8%	6.32	55.4%
P_m (N)	965	1274	32.0%	1780	84.5%
S_m (MPa)	4.07	5.37	32.0%	7.50	84.5%
G (J)	0.08	2.11	2540%	7.62	9430%

*The increase over the unreinforced cement specimen.

The load (P_1), flexural strength (S_1) and displacement (D_1) correspond to the first crack point, maximum load (P_m) and flexural strength (S_m), and toughness (G) are listed in Table 1. The points at which some of these mechanical quantities were measured are indicated in Fig. 5. Data from Table 1 show that the BSS wires are much more effective in improving the first crack displacement, the first crack and maximum strength and toughness of cement than CSS steel wires. The first crack strength, maximum strength and toughness of BSS steel wire reinforced cement are 26%, 40% and 260% higher, respectively than those of CSS steel wire reinforced cement.

3.2 Post Failure Observations

An examination of the post-test specimens can provide some insight on how the shape of the steel wires affects the mechanisms of crack initiation and propagation and crack bridging. Figure 6 shows that the unreinforced cement failed catastrophically by a single crack, which is virtually perpendicular to the longitudinal direction of the specimen. The blank cement fracture surfaces are flatter and smoother than those of the composite specimens are. Between the two composite types, the final fracture patterns are very different. Figure 7 shows a specimen reinforced with CSS steel wires, which also failed by a single crack. In contrast, multiple cracks initiated in BSS steel wire reinforced cement (Figure 8) along the tensile side of the specimen. Multiple matrix cracking before composite failure is similar to that observed in concrete reinforced with continuous steel re-bars under tensile stresses [1,31], further attesting the effectiveness of BSS wires in reinforcing cement. Figure 8 shows that multiple cracks are located along the longitudinal direction periodically with an average distance of 18 mm. This crack density is governed by the length and periodic arrangement of wires, as shown in Fig. 3, which produced periodic weak cross-sections of alternating aligned wire ends approximately spaced 18 mm apart (see Fig. 3).

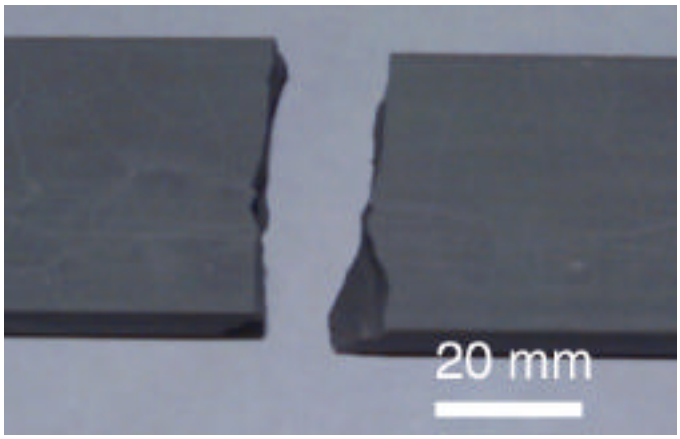

Figure 6. Photograph of the broken blank concrete specimen following four-point bending test.

In the BSS steel wire reinforced specimens, several secondary cracks developed and propagated at an angle with respect to the direction of the main crack. Branching of a propagating crack were perhaps promoted by the stress state created from microcracks formed at the enlarged wire ends and from the enlarged wire ends attempting to pull-out of the fracture surface. These secondary cracks were not observed in unreinforced cement

specimens and were observed in the CSS wire reinforced specimens only at the end of the test. In the unreinforced cement specimens, the central crack propagated catastrophically across the specimen. In the CSS wire specimen, the crack branched off in the horizontal direction at the end of the test, possibly caused by the debonded fiber-matrix interfaces ahead of the crack, shear stresses generated parallel to the top surface and alteration of the crack tip stress state by bridging of the main transverse crack by the CSS fibers.

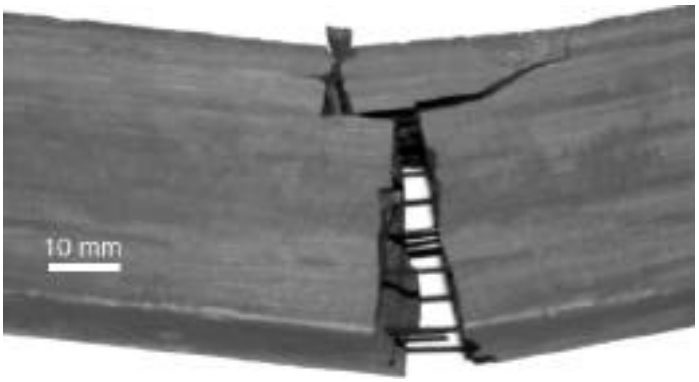

Figure 7. Photographs of the broken CSS steel wire reinforced concrete specimen after four-point bending test.

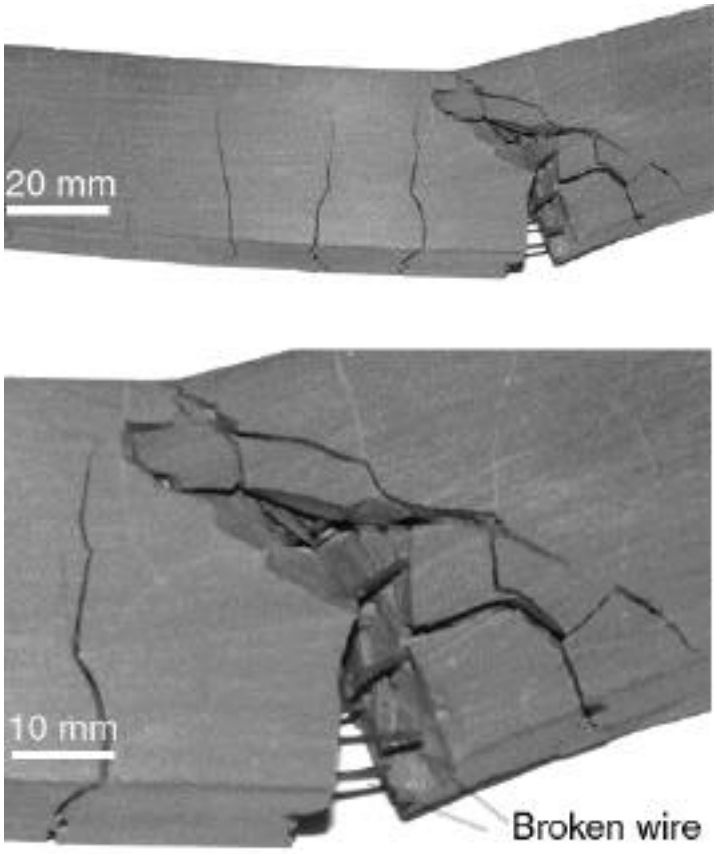

Figure 8. Photographs of the broken BSS steel wire reinforced concrete specimen following four-point bending test. A) multiple cracks and b) Magnified main crack.

The mechanical interlocking between the enlarged ends of BSS steel wires and matrix prevented most of the bridging BSS wires from pulling out and forced the wire to deform instead. As shown in Fig. 8, fracture occurred for most BSS steel wires and complete pull-out occurred for others, primarily those wires where one end was near the main crack surface**.** Therefore those BSS steel wires, which were well anchored into the matrix at both ends, could carry load and eventually deform plastically, work harden, and fail, a mechanism which significantly increased resistance to crack opening and propagation and the maximum strength of the composite. In contrast, nearly all CSS steel wires were easily pulled out without much deformation. The CSS steel wires depend on interfacial friction for crack bridging, which is not nearly as effective as the plastic deformation mechanism for BSS steel wires. Examining the stress-strain curve of the individual wires in Fig. 2, one can see that work hardening during the plastic deformation of steel wires further increases their load carrying capability. The total plastic deformation (12.6%) before failure consumes large amounts of energy. For those BSS wires that were pulled out, significant damage to the cement matrix occurred as a result. Furthermore, the main crack propagated in a tortuous way, which also consumed energy and enhanced the toughness.

3.3 Effective Wire Bridging.

Fiber bridging of a crack in concrete has been modeled by several researchers [21, 22, 27-29]. The discrete fiber bridging forces are usually treated as a continuous distribution of bridging forces (or stresses $\sigma(\delta)$) on the fracture surfaces of the crack. In the literature, two limiting configurations of bridged cracks in fiber composites have been developed. The first limit, the Aveston, Cooper, and Kelly (ACK) limit [30], is characterized by a long crack, entirely bridged by intact fibers. When the crack is long and the bridging fibers fail in the far wake, the linear elastic fracture mechanics or small scale bridging limit is reached. Under this condition, additional energy is supplied by these bridging forces. This bridging energy contribution, ΔG, can be calculated as the area under the bridging law [21, 27]

$$\Delta G = \int_0^{\delta_t} \sigma(\delta) d\delta \qquad (2)$$

where $\sigma(\delta)$ is the bridging law or stress acted on the crack by the bridging fiber at the total crack opening of δ. In Eq. (2), δ_t is the critical crack opening at the edge of the fiber bridging zone at which the ligament breaks (see Fig. 9a). Figure 9b illustrates hypothetical $\sigma(\delta)$ curves under various bridging conditions.

For both the CSS and BSS wire composites, the bridging zone appears to be approximately the same length and nearly equal to that of the specimen thickness. Therefore, it is likely that our four point bending specimens are too small to allow the bridging zone to fully develop. Therefore, it is unclear which of the two limiting configurations best approximates fracture in this cement-steel wire system. Despite this, the difference in the composite bending load versus displacement curves in Fig. 5 reflects those between the CSS and BSS wire bridging law $\sigma(\delta)$. Nonetheless, more informative studies on bridging mechanisms for different morphologies of wires will need specimen

configurations allowing for complete bridging zone development. Readers are referred to [28, 29,31] for more details on fiber bridging models for concrete composites.

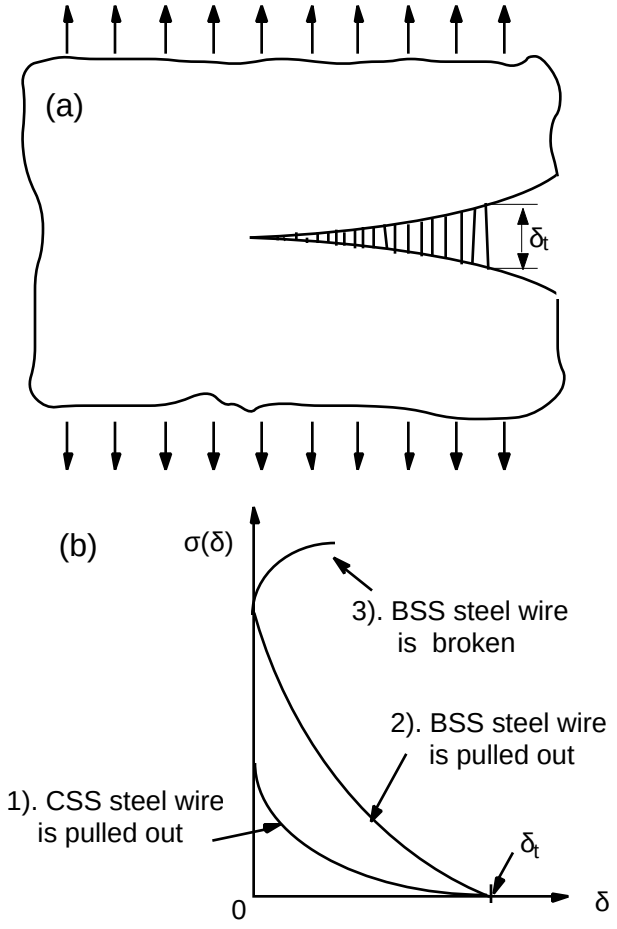

Figure 9. Schematic illustration of a) the crack-bridging zone and b) bridging stress-crack opening curves for three bridging situations.

The effectiveness of steel wires in improving toughness depends on both $\sigma(\delta)$ and δ_t (see Eq. 2). Based on the response of the CSS steel wire reinforced cement specimen after the first crack stress, we believe that the bridging stress $\sigma(\delta)$ provided by the CSS wires decreases monotonically with δ (see curve 1 in Fig. 9b) [21] as these CSS wires simply pull out of the matrix.

Depending on the fiber geometry and properties of the fiber and matrix, BSS fibers can either fracture or pull out in the wake of a propagating matrix crack. The overall bridging stress $\sigma(\delta)$ in either cases will most likely be higher than those of the CSS wires (see curves 2 and 3 in Fig. 9b). Consider first the case in which most BSS fibers are pulled out of the matrix. Due to their enlarged ends, BSS fibers require higher forces to be pulled out than the CSS wires. As shown in DCB fracture tests of a polyethylene reinforced polyester composite system, bridging BSS fiber composites had higher

resistance to crack opening than CSS fiber composites [16], even without fiber deformation and fracture. The higher resistance to pull out will result in higher bridging stresses, $\sigma(\delta)$, by BSS fibers (see curve 2 in Fig. 9b) than by CSS fibers.

Consider the second case wherein the BSS fibers fracture. If the wire is brittle and does not sustain much deformation before fracture, the crack bridging zone and δ_t could be very small, resulting in small ΔG as calculated using Eq. 2. On the other hand, if the wire is very ductile, as the steel wires used in this study, δ_t could be relatively large, and $\sigma(\delta)$ may take the shape of curve 3 in Fig. 9b.

As mentioned previously, for the BSS wire reinforced cement in this study, most of the bridging BSS wires were deformed to failure. As a result, the bridging law for the debonded BSS wire will be similar to that obtained from a wire tensile test with the crack opening displacement (plus debond length) acting as a gauge length. Therefore, the bridging stress $\sigma(\delta)$ will resemble curve 3 in Fig. 9b, in which the $\sigma(\delta)$ will be monotonically increasing over a longer range of δ in the bridging zone. However, other energy absorbing mechanisms can occur as well, like matrix cracking and debonding process, not accounted for in a simple tensile wire test.

Since the CSS bridging fibers were easily pulled-out and did not plastically deform, δ_t can be approximated as half of the fiber length or 12.5 mm. Since most BSS wires were monotonically strained to fracture, we calculate δ_t as the wire failure strain times wire length, which is 3.2 mm. Though δ_t is higher for the CSS case, the BSS steel wires are much more effective than the CSS steel wires at enhancing cement toughness, as shown in Fig. 5, because BSS wires render a much higher bridging force, $\sigma(\delta)$.

Lastly we mention that it was reported that the ends of BSS fibers promote *early* crack initiation in polyethylene fiber reinforced polyester matrix composites [16, 17]. This is not found in the BSS steel wire reinforced cement, as indicated by the higher first crack stress and displacement in the BSS wire reinforced specimen than in the CSS wire reinforced specimen.

4. Discussion and Recommendations

We have demonstrated in this paper the effectiveness of BSS steel wires in strengthening and toughening cement. The load-displacement curve for the BSS wire reinforced cement shown in Fig. 5 has many desirable characteristics for concrete infrastructures, such as a high stress plateau and strain-to-failure. However, it is likely that these results will not be common among all variations of BSS steel wire reinforced concrete. Namely the shape of the BSS fiber ends, fiber aspect ratio, volume content and distribution and interfacial properties are major factors that affect the mechanical properties of BSS steel reinforced concrete. Much modeling and experimentation are still needed to optimize these parameters for the best mechanical properties, such as strength and toughness. As with any fiber composite, in designing the optimal BSS wire concrete system, the interface, matrix, and fiber properties need to be accounted for together. There are complex interactions between these phases that govern the failure mechanisms that occur when the composite is stressed. For instance, if the matrix strain-to-failure is

substantially lower than that of the fiber, the matrix fails first and fibers are left to either break or bridge as an immediate response to the matrix cracks. Since the concrete-steel bond is relatively weak, the interface debonds, leaving the intact wire to bridge the matrix crack. The fibers bridging the crack are overloaded and can either break, pull-out, stretch or deform as the crack attempts to open up further under loading.

The BSS steel wires promote significant plastic deformation in bridging ligaments and the formation of multiple cracks, both of which consume more energy in fracture, and consequently improve composite toughness. When bridging matrix cracks, plastic deformation and work hardening of the steel wires plays a key role in obtaining high toughness and strength. In order to harness this response, we believe that there is a maximum enlarged end size to wire diameter ratio below which the fiber will not break. Also, for a given wire diameter and size of the enlarged ends, a minimum wire length is required for the wire to deform plastically and fracture instead of breaking the concrete matrix and being pulled out. This is because the wire needs to be embedded in the matrix for a certain depth in order to be held by the concrete matrix. A weak interface is also desired so that the wire debonds from the matrix, ideally over the length of the fiber minus the two ends, leaving an unconstrained section to deform and possibly neck before fracture. This will yield a larger δ_t and consume more energy. Multiple cracking is another effective mechanism for improving the composite toughness. As shown in Fig. 8, multiple cracks developed in the BSS-wire reinforced cement specimen. Distributed multiple cracking allows more bridging BSS wires to plastically deform.

Lastly, for a given length, there is a maximum volume fraction of wire above which it is difficult to achieve a uniform distribution of wires in concrete. Also there exists a minimum length below which the desirable multiple cracks will not be generated. A uniform distribution of the reinforcing steel wires in the matrix is important since clustered fiber ends will present weak spots where matrix cracks might initiate.

4. Conclusions and Future Work

Reinforcing cement using bone-shaped short (BSS) steel wires has been studied and proven to be more effective than using conventional straight short (CSS) steel wires. The first crack strength, maximum strength and toughness of BSS steel wire reinforced cement was 26%, 40% and 260% higher, respectively, than those of CSS steel wire reinforced cement. In this system, a substantial contribution to toughening was provided by the bridging BSS fibers, in the wake of the matrix crack, most of which plastically deformed to failure rather than pulling out. Therefore, if properly designed so that the majority of BSS wires undergo large plastic deformation and work hardening instead of pulling out, the BSS steel wire reinforced cement will be able to sustain high flexural stresses for a large deflection, i.e. significantly improving the toughness.

In both the BSS and CSS composites, matrix cracks diverted around the fibers, debonding the interface, indicating a low interfacial strength and matrix strain-to-failure, as compared to the strength of the steel wire. In four point bend testing, multiple cracks were generated in the BSS steel wire reinforced cement similar to that observed in continuous steel wire (or re-bar) reinforced concrete under tensile stresses [31]. In contrast, unreinforced and CSS wire reinforced specimens failed by a single central crack, with the former failing catastrophically. The multiple cracks generated in the BSS wire composite had smaller crack openings than the single crack in the other two specimen types. This also

further increased the overall toughness by allowing more steel wires to participate in crack-bridging and plastic deformation.

In this study, the cement matrix material did not contain aggregates, which tend to force cracks to follow tortuous, non-planar paths. The effectiveness of BSS steel wires in toughening concrete commonly used in civil infrastructures will be studied in future work. Also further studies, such as BSS wire pull-out tests and stochastic modeling of concrete fracture, is necessary to provide more insightful information on the roles of the geometry, volume fraction, and distribution of BSS wires on the mechanical properties of BSS-steel wire reinforced concrete. Lastly we suggest using larger specimens or an alternative specimen geometry, so that the bridging zone may fully develop and important bridging mechanisms may be better understood and modeled for this BSS system. In doing so, it is crucial to keep in mind that fiber composites and brittle materials, such as aggregate concrete, are well known to exhibit size effects; that is, the strength decreases with size [31].

Acknowledgment

The authors thank Mr. M. L. Lovato and R. W. Ellis for their assistance in mechanical testing and photographing. Support was provided by the Laboratory Directed Research and Development Office of Los Alamos National Laboratory. This work was performed at Los Alamos National Laboratory under the auspices of the U.S. Department of Energy (contract W-7405-ENG-36).

References

1 ACI Committee 544, Fiber Reinforced Concrete, American Concrete Institute, Farmington Hills, Michigan, 1997.
2. Shah SP. Do fibers increase the tensile strength of cement bases composites? ACI Materials Journal, 1991; 88:595-602.
3. Naaman AE. Fiber reinforcement of concrete. Concrete International: Design and Construction 1985; 7:21-25.
4 ACI Committee 544, Revision of state-of-the-art report (ACI 544 TR-73) on fiber reinforced concrete, ACI journal, Proceedings 1973; 70:727-744.
5 Oh B., Lim D., Hong K., Yoo S., and Chae S. Structural Behavior of Steel fiber Reinforced Concrete Beams in Shear. In: Banthia N., MacDonald C. and Tatnall P, editors, Structural Applications of Fiber Reinforced Concrete. ACI SP-182. ACI, Farmington Hills, Michigan, 1999.pp. 9-19.
6. Casanova P. and Rossi P. High Strength Concrete Beams Submitted to Shear: Steel Fibers Versus Stirups. In: Banthia N., MacDonald C. and Tatnall P, editors, Structural Applications of Fiber Reinforced Concrete. ACI SP-182. ACI, Farmington Hills, Michigan, 1999.pp. 53-67.
7. Campione G. and Mindess S. Compressive Toughness Characterization of Normal and High-Strength Fiber Concrete Reinforced with Steel Spiral. In: Banthia N., MacDonald C. and Tatnall P, editors, Structural Applications of Fiber Reinforced Concrete. ACI SP-182. ACI, Farmington Hills, Michigan, 1999.pp. 141-161.
8. Kelly A. Strong Solids, 2nd edition (Oxford University Press, Oxford, 1973).
9. Briggs A. Carbon Fiber Reinforced Cement. J. Mater. Sci., 1977; 12:384-404.

10. Alford N. McN. and Birchall JD., Fiber Toughening of MDF Cement. J. Mater. Sci., 1985; 20:37-45.
11. Baggott R. and Gandhi D. Multiple Cracking in Aligned Polypropylene Fiber Reinforced Cement Composites. J. Mater. Sci., 1981; 16:65-74.
12. Balagaru PN. and Shah SP., Fiber-Reinforced Cement Composites, McGraw-Hill, New York, p. 530 (1992).
13. Kim T.-J., and Park C.-K. Flexural and Tensile Strength Developments of Various Shape Carbon-Fiber-Reinforced Light Weight Cementitious Composites, Cement and Concrete Research, 1998; 28:955-960.
14. Fiber Reinforced Concrete, Reported by ACI Commmittee 544. ACI 544.1 R-96.
15. Daniel JI., Roller JJ., Litvin A., Azizinamini A. and Anderson ED. Fiber Reinforced Concrete, SP 39.01T, Portland Cement Association, Skokie, 1991.
16. Zhu YT., Valdez JA., Beyerlein IJ., Zhou S., Liu C., Stout MG., Butt DP., and Lowe TC. Mechanical Properties of Bone-Shaped-Short-Fiber Reinforced Composites, Acta Materialia, 1999; 47:1767-1781.
17. Zhu YT., Valdez JA., Shi N., Lovato ML., Stout MG., Zhou S., Blumenthal WR., and Lowe TC. Influence of Reinforcement Morphology on the Mechanical Properties of Short-Fiber Composites, Processings of Metals and Advanced Materials: Modeling, Design and Properties. Edited by B. Q. Li, TMS, 1998, pp. 251-259.
18. Zhu YT., Valdez JA., Shi N., Lovato ML., Stout MG., Zhou S., Blumenthal BR., and Lowe TC., A Composite Reinforced with Bone-Shaped Short Fibers," Scripta Materialia, 1998; 38:1321-1325.
19. Zhu YT., Beyerlein IJ., Valdez JA., and Lowe TC. Fracture Toughness of a Composite Reinforced with Bone-Shaped Short Fibers, submitted to Materials Science and Engineering A.
20. Avery C. Concrete Construction & Estimating, Craftsman Book Company, Solana Beach, CA, 1975. pp 355-382.
21 Visalvanich K. and Naaman AE.. Fracture model for fiber reinforced concrete. ACI Journal, 1983; 80:128-138.
22. Stang H. and Shah SP. Failure of fiber-reinforced composites by pull-out fracture. J. Mater. Sci. 1986; 21:953-957.
23 Gopalaratnam VS., Asce AM., Shah, SP., and Asce, M. Tensile failure of steel-reinforced Mortar, J. Eng. Mech. 1987; 113[5]:635-653.
24. Chau PS. and Piggott MR. The glass fiber-polymer interface: I–theoretical consideration for single fiber pull-out tests. Comp Sci Tech. 1985; 22:33-42.
25 Wang C. Fracture mechanics of single-fiber pull-out test. J. Mater. Sci., 1997; 32:483-490.
26. ASTM standard C 1341-97.
27 Jenq YS., Asce SM., Shah SP. and Asce M., Crack Propagation in Fiber Reinforced Concrete, J. Structural Engineering, 1986; 112:19-34.
28 Lenain JC. and Bunsell AR. The Resistance to Crack Growth of Asbestos Cement," J. Mater. Sci., 1979; 14:321-332.
29. Bowling J. and Groves GW. The Propagation of Cracks in Composites Consisting of Ductile Wires in a Brittle Matrix," J. Mater. Sci., 1979; 14:443-449.
30. Aveston, J., Cooper, G.A., and Kelly, A. Single and multiple fracture, in *The properties of fiber composites,* Conf. Proc. National Physics Laboratory, IPC Science and Technology Press Ltd., 1971; 15.
31. Bazant, Z. and Planas, J. Fracture and size effect in concrete and other quasibrittle materials. New York: CRC LLC Press, (1998).